CANCER

Therapeutic synergy between tigecycline and venetoclax in a preclinical model of *MYC/BCL2* double-hit B cell lymphoma

Micol Ravà,[1,2]* Aleco D'Andrea,[1]*† Paola Nicoli,[1] Ilaria Gritti,[1]‡ Giulio Donati,[1] Mirko Doni,[1] Marco Giorgio,[1] Daniela Olivero,[3] Bruno Amati[1,2]§

High-grade B cell lymphomas with concurrent activation of the *MYC* and *BCL2* oncogenes, also known as double-hit lymphomas (DHL), show dismal prognosis with current therapies. *MYC* activation sensitizes cells to inhibition of mitochondrial translation by the antibiotic tigecycline, and treatment with this compound provides a therapeutic window in a mouse model of *MYC*-driven lymphoma. We now addressed the utility of this antibiotic for treatment of DHL. *BCL2* activation in mouse Eμ-*myc* lymphomas antagonized tigecycline-induced cell death, which was specifically restored by combined treatment with the BCL2 inhibitor venetoclax. In line with these findings, tigecycline and two related antibiotics, tetracycline and doxycycline, synergized with venetoclax in killing human *MYC/BCL2* DHL cells. Treatment of mice engrafted with either DHL cell lines or a patient-derived xenograft revealed strong antitumoral effects of the tigecycline/venetoclax combination, including long-term tumor eradication with one of the cell lines. This drug combination also had the potential to cooperate with rituximab, a component of current front-line regimens. Venetoclax and tigecycline are currently in the clinic with distinct indications: Our preclinical results warrant the repurposing of these drugs for combinatorial treatment of DHL.

INTRODUCTION

High-grade B cell lymphomas with *MYC* and *BCL2* or *BCL6* translocations, hereby referred to as double-hit lymphomas (DHL), constitute a subset of diffuse large B cell lymphoma (DLBCL) that was recently reclassified as a separate entity (*1*–*4*). Additional cases of DLBCL, commonly referred to as double-expressors, show positivity for the MYC and BCL2 proteins in the absence of the corresponding translocations. In both groups, activation of MYC and BCL2 correlates with poor prognosis in the face of current front-line treatments, including combined immunotherapy and chemotherapy [such as rituximab and CHOP (cyclophosphamide, doxorubicin, vincristine, and prednisolone) chemotherapy, or R-CHOP] (*1*–*7*), calling for the development of new therapeutic regimens. A most promising prospect in this regard is the emergence of selective BCL2 inhibitors, such as venetoclax (also called ABT-199) (*3*, *8*–*10*).

The synergy between *MYC* and *BCL2* in lymphomagenesis was originally demonstrated in transgenic mice (*11*, *12*) and is explained by the ability of BCL2 to block the proapoptotic activity of MYC while leaving its proliferative potential intact (*13*–*15*). On this basis, we reasoned that compounds that exacerbate MYC-induced apoptosis would be likely to cooperate with venetoclax in killing DHL cells. A candidate compound was tigecycline (*16*, *17*), a broad-spectrum antibacterial agent with documented cytotoxicity against diverse cancer cell types, most likely owing to its inhibitory effect on mitochondrial translation (*18*).

Genes encoding components of the mitochondrial ribosome were coordinately activated during lymphomagenesis (*19*) and were critical for tumor maintenance in Eμ-*myc* transgenic mice (*16*). In line with these genetic data, pharmacological inhibition of the mitochondrial ribosome with tigecycline was synthetically lethal with *MYC* activation, impaired tumor cell survival in vitro, and extended life span in lymphoma-bearing mice (*16*, *17*). Here, we present preclinical data showing that venetoclax and tigecycline synergize in the treatment of *MYC/BCL2* DHL, allowing tumor eradication in xenografted mice.

RESULTS

Tigecycline-induced apoptosis is suppressed by BCL2 and restored by venetoclax

Tigecycline-induced cell death in mouse Eμ-*myc* lymphoma cell lines (*16*) was suppressed upon infection of the cells with a BCL2-expressing retrovirus (Fig. 1A and table S1). Under these conditions, tigecycline suppressed proliferation, with concomitant G_1 arrest and induction of the cell cycle–inhibitory gene *Cdkn1a* (Fig. 1B and fig. S1, A and B). This antiproliferative effect was independent from the p53 status of the tumors and was not associated with appearance of the senescence-associated marker SA-βgal (senescence-associated β-galactosidase), unlike observed with doxorubicin (fig. S1C) (*20*). Thus, BCL2 blocked the apoptotic effect of tigecycline without affecting its cytostatic action.

As seen with tigecycline, Eμ-*myc*/*BCL2* lymphomas were resistant to venetoclax alone (Fig. 1C) but were killed by the two drugs together, with strong dose-dependent and synergistic effects (Fig. 1D, fig. S1D, and table S1). This combined toxicity was p53-independent, as previously shown for tigecycline-induced cell death (*16*). The action of venetoclax was on target because Eμ-*myc* lymphomas expressing BCL-W, a BCL2-related antiapoptotic protein that is not inhibited by venetoclax (*8*), were resistant to the combined treatment (fig. S1E and table S1). Hence, venetoclax specifically restored tigecycline-induced cell death in Eμ-*myc*/*BCL2* lymphomas.

Tigecycline and venetoclax cooperate in killing human DHL cell lines

We then addressed the effect of the drugs on five human *MYC/BCL2* DHL cell lines, in which we first confirmed the expression of either

[1]Department of Experimental Oncology, European Institute of Oncology, Via Adamello 16, 20139 Milan, Italy. [2]Center for Genomic Science of IIT@SEMM, Fondazione Istituto Italiano di Tecnologia, Via Adamello 16, 20139 Milan, Italy. [3]Laboratorio Analisi Veterinarie BiEsseA, Via A. d'Aosta 7, 20129 Milan, Italy.
*These authors contributed equally to this work.
†Present address: QuintilesIMS, Via Roma 108, 20060 Cassina de' Pecchi, Milan, Italy.
‡Present address: Functional Genomics of Cancer Unit, Division of Experimental Oncology, Istituto San Raffaele, 20132 Milan, Italy.
§Corresponding author. Email: bruno.amati@ieo.it

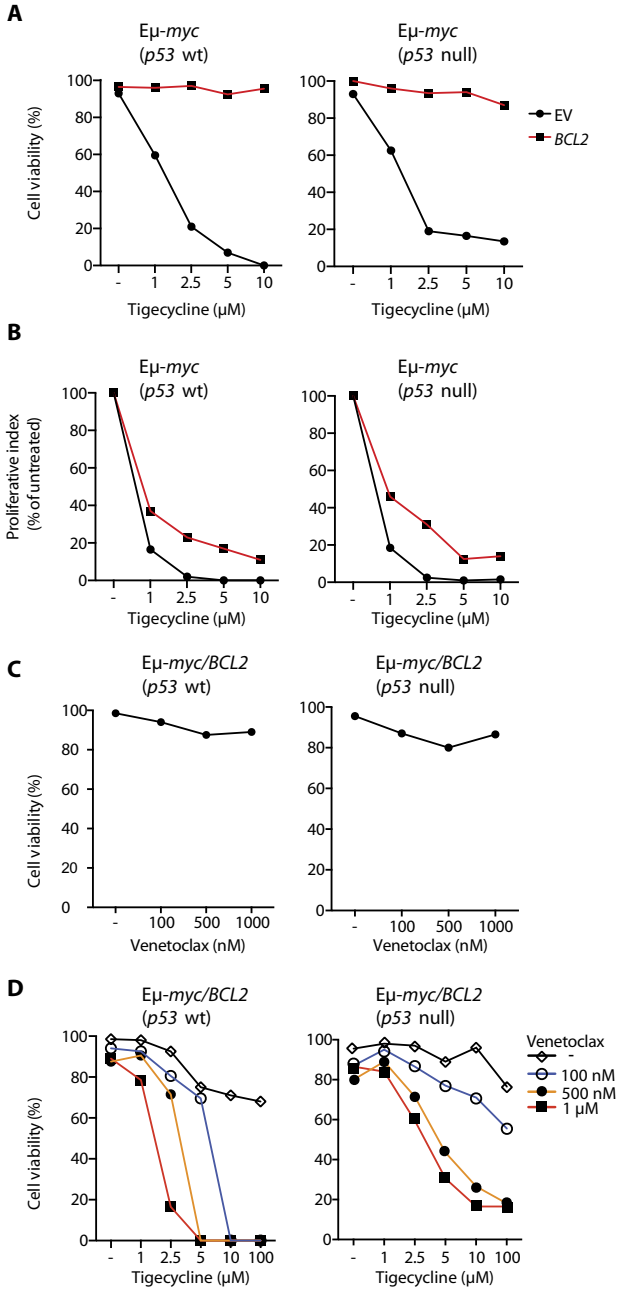

Fig. 1. Blockade of tigecycline-induced cell death by BCL2 in Eμ-*myc* lymphomas and its restoration by venetoclax. Two mouse Eμ-*myc* lymphomas, one wild type (p53 wt) and one null (p53 null), for the Trp53 locus were infected with a recombinant retrovirus encoding human BCL2 or with the corresponding empty vector (EV). After selection, the infected cells were treated with tigecycline and/or venetoclax at the indicated concentrations. Total and viable cell counts were determined by Trypan blue exclusion 48 hours after addition of the drugs to the culture medium. (**A**) The viability of cells expressing BCL2 or EV is presented as the percentage of live relative to total cells (live + dead) in each culture. (**B**) The proliferative index of cells expressing BCL2 or EV is presented as the increase in viable cell counts over 48 hours, normalized to the corresponding increase in parallel untreated cultures (4 population doublings for the p53 wt cells with either EV or BCL2; 3.5 and 2 doublings for the p53 null cells with EV and BCL2, respectively). (**C**) Cell viability of Eμ-*myc/BCL2* lymphomas in the presence or absence of venetoclax. (**D**) Cell viability of Eμ-*myc/BCL2* lymphomas in the presence or absence of tigecycline and/or venetoclax. All data points represent the average ± SD from three independent experiments.

oncogene (Fig. 2, A and B). In three of these lines (Karpas-422, SU-DHL-6, and DOHH-2), neither tigecycline nor venetoclax alone showed significant proapoptotic activity, but the two drugs synergized when combined (Fig. 2C, fig. S2, and table S1). In two others (SU-DHL-4 and OCI-LY8), venetoclax alone showed dose-dependent toxicity, but this was still enhanced by the addition of tigecycline. Finally, a DLBCL line with activation of *MYC*, but not of *BCL2* (OCI-LY7), was fully resistant to the combination, implying that the effect of venetoclax was, once again, on target (and, incidentally, that OCI-LY7 cells must carry a different antiapoptotic lesion). Thus, as in mouse Eμ-*myc*/BCL2 lymphomas, tigecycline and venetoclax cooperated in killing human DHL lines.

The toxicity of tigecycline and related antibiotics to tumor cells (either rodent or human) has been associated with their inhibitory effect on mitochondrial translation and, hence, on respiratory activity (*16*, *18*, *21*–*31*). Consistent with this notion, treatment of SU-DHL-6 cells with tigecycline, doxycycline, or tetracycline suppressed expression of the mitochondrion-encoded electron transport chain complex (ETC) IV subunits cyclooxygenase 1 (COX1; or MTCO1) and COX2 (or $MTCO_2$) but not of the nucleus-encoded ETC II subunit SDHA (fig. S3A) and lowered oxygen consumption (fig. S3B). Finally, doxycycline and tetracycline also synergized with venetoclax in killing SU-DHL-6 cells (fig. S3C and table S1). Hence, concomitant inhibition of mitochondrial translation and of the prosurvival function of BCL2 allows effective killing of DHL cells.

Tigecycline and venetoclax allow eradication of DHL-derived tumors in mice

To address the therapeutic potential of tigecycline and venetoclax, we xenografted the human DHL cell lines SU-DHL-6, DOHH-2, and OCI-LY8 in CD1-nude mice, let tumors develop for 2 weeks, and initiated treatment. Either drug alone partially slowed down tumor progression, but their combination showed strong antitumoral activity, causing either full regression (eight of eight for SU-DHL-6 and three of nine for OCI-LY8) or stasis within the 12 days of treatment (Fig. 3 and table S1). The contribution of venetoclax was again on target because BCL2-negative OCI-LY7 tumors were resistant to the combination. Immunohistochemical analysis of SU-DHL-6 tumors after 1 day of treatment showed decreased cell cohesiveness and intratumoral necrosis with the combined drugs, associated with proliferative arrest and apoptosis (fig. S4). Follow-up of the animals upon cessation of treatment showed that OCI-LY8 and DOHH-2 tumors regrew over relatively short periods of time, requiring sacrifice of the animals within about 1 month (Fig. 3 and table S1). Instead, most of the SU-DHL-6–xenografted animals remained tumor-free until our preset end point (120 days) and could thus be considered as cured (Table 1).

Mice sacrificed either after long-term survival with the highest doses of the combined drugs (day 120) or after short-term treatment with tigecycline alone (day 19) revealed a compacted liver morphology (Table 1 and fig. S5A, day 120). Histological analysis (performed at day 19) showed that this morphological change was associated with a thickening of the liver capsula and peritoneal membrane (fig. S5B). This was most likely a reactive lesion secondary to the twice-a-day intraperitoneal injection of tigecycline because it was absent after intravenous injection, the relevant route in the clinic (*32*), whereas both modalities were equally effective in slowing down tumor progression (fig. S5C and table S1). Peripheral blood profiles revealed no significant alterations in cell populations in treated versus untreated animals (at day 12; fig. S5D). Combined treatment caused an increase in alanine aminotransferase activity (fig. S5E), consistent with liver injury, albeit without

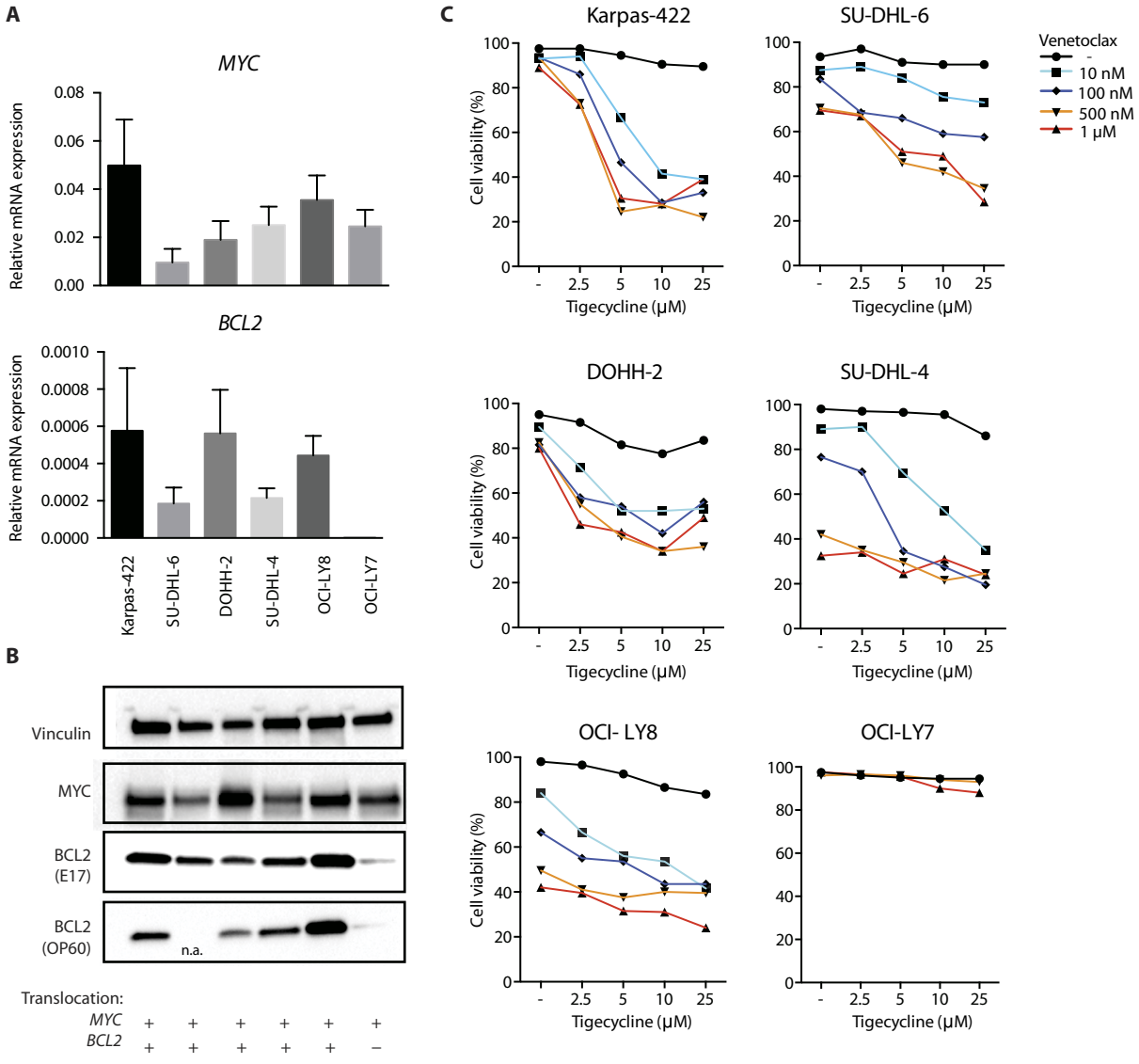

Fig. 2. Induction of cell death by tigecycline and venetoclax in human *MYC/BCL2* DHL. (**A** and **B**) *MYC* and *BCL2* mRNAs were quantified by RT-PCR (reverse transcription polymerase chain reaction) with normalization to the *RPLP0* mRNA ($n = 3$ technical replicates for each group) (A) or immunoblotting (B) in the indicated cell lines. The expression data shown here are consistent with the known status of *MYC* or *BCL2* translocations in those cell lines, as indicated at the bottom. Note that in SU-DHL-6 cells, somatic mutations in BCL2 impair its recognition by the OP60 antibody (n.a.) (*65*), but the protein is readily detected by antibody E17. (**C**) Cultures were treated with tigecycline and/or venetoclax at the indicated concentrations, and cell viability was determined as in Fig.1.

overt signs of toxicity such as necrosis or fibrosis (fig. S5B). Treated animals were overall in good health, and histopathological analysis showed no alterations in the major organs, with the exception of inflammatory infiltrates in the liver and spleen in the presence of tigecycline (alone or in combination) (fig. S6). Finally, we note that a fraction of the mice treated with high doses of the combined drugs died within 1 week (Table 1). Although the causes underlying this effect remain to be addressed, lower dosage [tigecycline (75 mg/kg) and venetoclax (50 mg/kg)] showed no toxicity yet retained substantial antitumoral effects.

Tigecycline and venetoclax synergize against a DHL patient-derived xenograft

A recent study described the establishment of DLBCL patient-derived xenografts (PDXs), some of which were classified as DHL (*33*). We expanded one of these PDX lines (DFBL-69487-V3-mCLP, expressing luciferase) in NSG mice and assessed its response to treatment. Cell suspensions (1×10^6) were transferred intravenously into the recipient mice, and tumor development was monitored by whole-body imaging. Groups were randomized after 2 weeks (day 0), and treatment was applied as above (days 1 to 12). Although they slowed down tumor progression, either tigecycline or venetoclax alone were insufficient to reverse the course of disease. In contrast, the combination caused rapid and marked tumor regression: In particular, luminescence in the femur (f.) and vertebrae (v.), detectable in the controls, was suppressed by about two orders of magnitude or became undetectable altogether between days 11 and 19 in double-treated animals (Fig. 4, A and B, table S1, and fig. S7). However, tumors were not eradicated and regrew at variable rates after cessation of treatment (Fig. 4A, table S1, and fig. S7,

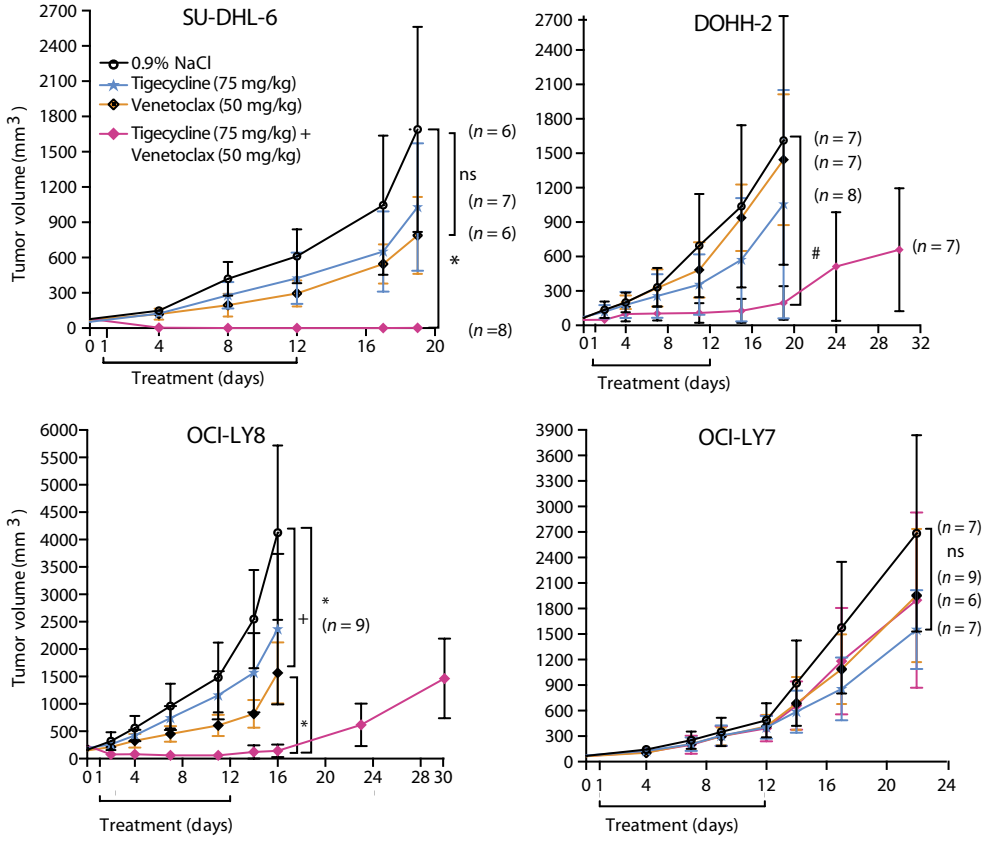

Fig. 3. Therapeutic activity of tigecycline and venetoclax in DHL-xenografted mice. The human cell lines SU-DHL-6, DOHH-2, OCI-LY8 (all with *MYC* and *BCL2* translocations), or OCI-LY7 (*MYC* translocation only) were xenografted subcutaneously in CD1-nude mice. After about 2 weeks, tumor-bearing animals were randomized and treated with the indicated doses of tigecycline and/or venetoclax over a period of 12 days. Tumor volumes were measured at the indicated time points after treatment. For DOHH-2, OCI-LY8, and OCI-LY7, tumor growth is shown at every time point until termination. For SU-DHL6 tumors, only days 0 to 19 are included in the graph: Of the eight animals treated with tigecycline + venetoclax, six reached the 120-day end point tumor-free, and two developed tumors and were sacrificed at day 50 (table S1). Error bars represent SD; $^{\#}P = 5 \times 10^{-3}$, $^{+}P < 5 \times 10^{-4}$, and $^{*}P < 10^{-5}$; ns, not significant.

days 19 to 29). Taking disease manifestation (hindlimb paralysis and hunched posture) as the end point, untreated and single drug-treated animals had to be sacrificed at day 24, whereas combination-treated animals reached day 48 (fig. S8). Thus, as observed above with the cell lines, tigecycline and venetoclax showed strong antitumoral effects with the DHL-derived PDX.

Tigecycline cooperates with rituximab

The anti-CD20 monoclonal antibody rituximab is a component of R-CHOP, the front-line immunochemotherapeutic regimen used to treat patients with DLBCL. However, those tumors that show *MYC* and *BCL2* translocations, thus qualifying as DHL, show poor primary responses and high rates of relapse (*2*–*7*). In mice bearing SU-DHL-6 tumors, rituximab showed cooperation with either tigecycline or venetoclax in slowing tumor growth (fig. S9A and table S1; compare with Fig. 3 for tigecycline or venetoclax alone). However, the strong effect of tigecycline and venetoclax together precluded clear conclusions on an added advantage of rituximab. In DOHH-2 tumors, rituximab cooperated neither with tigecycline nor with venetoclax: The latter appears in contrast with a previous report (*8*) but may be due to the lower dosage of venetoclax used in our experiment (50 mg/kg versus 100 mg/kg daily). Nevertheless, when added as a third component on top of tigecycline and venetoclax, rituximab retarded the regrowth of DOHH-2 tumors (fig. S9A, 16 and 20 hours, and table S1). Finally, in PDX-recipient mice, rituximab showed moderate cooperation with either tigecycline or venetoclax, although its effect on the two-drug combination was not statistically significant (figs. S9, B and C, and S10). Hence, besides providing synergy against DHL as a two-drug combination, as shown in the previous sections, tigecycline and venetoclax have the potential to reinforce rituximab-containing therapies in the clinic.

DISCUSSION

Among B lymphoid malignancies, DHL with concurrent *MYC* and *BCL2* translocations (recently reclassified as high-grade B cell lymphomas) (*1*) show the poorest prognosis. Hence, the development of additional therapeutic strategies represents a critical unmet need for patients who recur with this class of lymphomas (*2*–*7*). Previous work showed that *MYC* activation sensitized cells to tigecycline and that treatment with this antibiotic retarded the progression of *MYC*-driven lymphomas in mice (*16*, *17*). Here, we followed up on these findings to assess the activity of tigecycline against DHL, in combination with the BCL2 inhibitor venetoclax (*8*–*10*). We first showed that overexpression of BCL2 in mouse Eμ-*myc* lymphomas blocked tigecycline-induced cell death, which was restored upon

Table 1. Summary of all treatments performed on mice with SU-DHL-6–derived tumors. *n* mice (died ≤1 week) refer to the total numbers of mice treated and, in parentheses, those that died within the first week. The causes for these early deaths remain unclear and may be due to the overall experimental burden imposed on the animals; surviving animals showed no signs of distress. Regression: Percentages of animals scored as showing tumor regression at the indicated time points, with the scored/total numbers in parentheses. At day 19, partial and complete regressions were defined as residual tumor volumes ≤50% and ≤10% of the initial volume, respectively. Animals showing complete regression at day 19 were followed until day 120 and sacrificed when tumors reached a diameter of 2 cm. Animals reaching the end point of 120 days had no detectable residual tumor. Compacted liver: "Yes" indicates that the postmortem examination revealed a compacted liver lobule morphology.

Tigecycline, mg/kg	Venetoclax, mg/kg	*n* mice (died ≤1 week)	Regression: % tumor-free (*n*)			Compacted liver
			Day 19: Partial	Day 19: Complete	Day 120	
0.9% NaCl	—	14	—	—	—	—
—	Vehicle	13	—	—	—	—
75	—	7	—	—	—	Yes
100	—	12	—	—	—	Yes
—	25	14	—	—	—	—
—	50	6	—	—	—	—
—	100	7	—	—	—	—
100	100	7 (3)	—	75% (3/4)	75% (3/4)	Yes
100	50	6		100% (6/6)	100% (6/6)	Yes
100	50	10 (2)	12.5% (1/8)	87.5% (7/8)	50% (4/8)	Yes
100	25	7	57% (4/7)	—	—	Yes
75	100	10 (5)	20% (1/5)	80% (4/5)	60% (3/5)	Yes
75	100	8 (3)		100% (5/5)	60% (3/5)	Yes
75	50	8	12.5% (1/8)	87.5% (7/8)	75% (6/8)	Yes
50	50	7	—	100% (7/8)	42% (3/7)	—
25	100	7	—	28% (2/7)	—	—

coexposure to venetoclax. Consistent with this finding, the two drugs synergized in killing human DHL cells in vitro and showed strong antitumoral activity in vivo in mice xenografted with DHL cell lines or a PDX. With one line in particular (SU-DHL-6), the combined treatment achieved full disease eradication.

The antitumoral activity of tigecycline in either mouse or human cells is attributed to its inhibitory activity on mitochondrial translation and, as a consequence, on oxidative phosphorylation (*16*, *18*, *25*–*31*). Other antibiotics with similar properties were also toxic toward a variety of tumor cells (*21*–*25*) and, as shown here for doxycycline and tetracycline, cooperated with venetoclax in killing DHL cells. Tigecycline was also reported to inhibit WNT/β-catenin (*34*) and PI3K (phosphatidylinositol 3-kinase)–AKT–mTOR (mammalian target of rapamycin) signaling (*30*, *35*, *36*) and to induce AMP-activated protein kinase (AMPK) signaling and autophagy (*36*, *37*), but these effects may conceivably follow from mitochondrial dysfunction. Hence, although tigecycline and related antibiotics may inhibit other activities in eukaryotic cells, a comprehensive body of evidence points to the mitochondrial ribosome as their direct and critical target. The reciprocal is true as well because compounds isolated as mitochondrial ribosome inhibitors also showed antibacterial activity (*38*).

A recent study suggested that the sensitivity of several DLBCL cell lines to tigecycline was determined by their classification within the OxPhos as opposed to the B cell receptor (BCR) subtype (*39*), as defined by gene expression profiling (*40*). However, one of the OxPhos lines (Karpas-422) was resistant to tigecycline alone in our experiments (and was also the least sensitive of the OxPhos lines in the previous study). We also note that OxPhos/BCR are secondary to the alternative cell-of-origin–based signatures in the clinic (activated and germinal center B cell–like) and that, regardless of these expression-based classifications, DLBCL cases show heterogeneous mutational landscapes (*41*, *42*). Altogether, the determinants of tigecycline sensitivity, as well as its full molecular and metabolic effects in lymphomas, remain to be fully characterized. This notwithstanding, the synergy with venetoclax reported here should be selective for *MYC/BCL2* double-hit, and possibly double-expressor, lymphomas (*3*).

In the clinic, tigecycline is among the antibiotics indicated for treatment of opportunistic, multidrug-resistant infections in cancer patients, with promising antibacterial responses and safety profiles (*43*–*47*). However, in this setting, tigecycline's possible contribution to antitumoral responses was not considered. On the basis of the preclinical effect of tigecycline against acute myeloid leukemia (AML) (*26*, *48*), a phase 1 study was undertaken in patients with relapsed AML (*32*), but no clinical response was reached so far, highlighting the need to reconsider the formulation and dosage of the antibiotic (*32*, *49*), as well as its possible activity in combination regimens.

Preclinical studies reported that tigecycline cooperates with chemotherapeutic drugs in hepatocellular and renal cell carcinomas (*29*, *30*), as well as with the BCR-ABL kinase inhibitor imatinib in chronic myelogenous leukemia, where it contributed to the eradication of stem/progenitor cells (*31*), a feature that was independently reported for venetoclax (*50*, *51*). Tigecycline also targeted cancer stem cells (CSCs) in AML (*26*), breast, and other tumor types (*25*, *28*), pointing to a critical function of mitochondrial translation in CSCs. Other studies

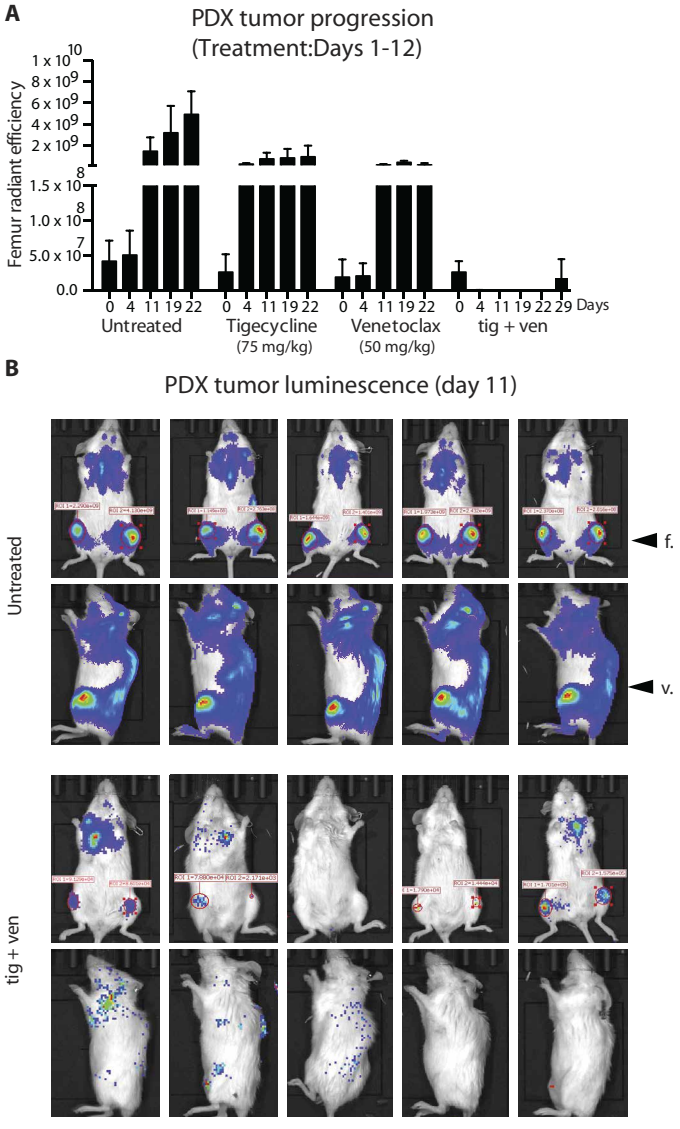

Fig. 4. Therapeutic activity of tigecycline and venetoclax in a DHL patient-derived xenograft. The patient-derived xenograft line DFBL-69487-V3-mCLP, expressing luciferase, was expanded by intravenous injection in NSG mice. Fifteen days after seeding (day 0), tumor development was monitored by whole-body imaging: Animals were randomized (five animals per group), subjected to treatment with tigecycline (75 mg/kg) and/or venetoclax (50 mg/kg) over a period of 12 days (days 1 to 12), and monitored by whole-body imaging at the indicated time points (before, during, and after treatment). (**A**) Tumor progression in the indicated groups of animals was followed by radiant efficiency, quantified over both femurs. (**B**) IVIS imaging (ventral and lateral) of all mice in the control (untreated) and tigecycline + venetoclax (tig + ven) groups, shown at day 11. Other groups and time points are shown in fig. S7A. Arrowheads point to the accumulation of tumor cells in the femurs (f.) and vertebrae (v.). The red circles and rectangles appearing over the photographs define the areas that were used for quantification of luminescence over the femur and the corresponding values, respectively. All values are provided in table S1.

indicated that mitochondrial electron transport is critical for the survival of CSCs or cancer-repopulating cells (*52*, *53*) and may itself be suppressed upon BCL2 inhibition (*53*, *54*). Finally, MYC and the BCL2-related protein MCL1 cooperated to promote mitochondrial respiratory activity and chemotherapy resistance in breast CSCs (*55*). Together with our data in DHL, these observations suggest that tigecycline and venetoclax (or other BH3-mimetic drugs) (*15*) may complement current therapeutic regimens in a variety of tumor types.

Multiple clinical studies have addressed the safety and efficacy profiles of venetoclax against hematological malignancies (*10*, *56*–*61*), including lymphoma (*57*). Compared with other subtypes of lymphoma, venetoclax appears to be relatively ineffective against DLBCL (*3*, *10*), although the impact of the *MYC*/*BCL2* status on clinical responses was not reported. Venetoclax showed cooperativity with rituximab in patients with chronic lymphocytic leukemia (*58*, *61*), as well as in mice xenografted with DHL cell lines (*8*), as confirmed in our work. Finally, and most relevant for future clinical development, the effects of venetoclax and tigecycline in either DOHH-2 or PDX-derived tumors appeared to be reinforced by the addition of rituximab in our study.

In conclusion, our preclinical data have uncovered a synergy between tigecycline and venetoclax against DHL, warranting the repurposing of these drugs in combination for secondary treatment of patients with refractory or relapsed *MYC/BCL2* DHL. Moreover, the addition of both compounds to R-CHOP or other rituximab-based chemoimmunotherapeutic regimens (*3*) may improve the primary response of patients with this particularly aggressive lymphoma subtype.

MATERIALS AND METHODS

Study design

The objective of our study was to address the therapeutic interaction between tigecycline and venetoclax against *MYC/BCL2* DHL in a preclinical setting. For in vivo pharmacological studies, human DHL cell lines and PDX were xenotransplanted in female CD1-nude and NSG mice, respectively. Tumors were allowed to develop to measurable sizes (about 2 weeks), followed by exclusion of outliers, blinded randomization of the experimental groups (day 0), and treatment (days 1 to 12), as described in detail below. Although the number of biological replicates achieved depended on the efficiency of engraftment and tumor growth, no fewer than four to five animals were included in any experimental group (with the exception of fig. S5C) to ensure statistical power. The end point of the experiment for subcutaneous tumors (with the DHL cell lines) was either a tumor size of 20 mm in any one dimension or ulceration at any tumor size. For PDX-derived tumors, the end point was the first signs of disease manifestation (hindlimb paralysis and hunched posture). The data used for every graph in our figures are reported in table S1.

Cell lines

The Eμ-*myc* p53-wt and p53-null lymphoma lines used here, LY27 and LY35, respectively, were the same as in our previous work and were cultured as described therein (*16*). The human lymphoma lines DOHH-2 and Karpas-422 were cultured in RPMI 1640 supplemented with 10% fetal bovine serum, 2 mM L-glutamine, and 1% penicillin/streptomycin. The lines SU-DHL-4, SU-DHL-6, OCI-LY7, and OCI-LY8 were cultured in Iscove's modified Dulbecco's medium with the same supplements. The information on *BCL2* and *MYC* translocation reported in Fig. 2B was obtained from either American Type Culture Collection (www.lgcstandards-atcc.org/Products/Cells_and_Microorganisms/Cell_Lines/Human.aspx) or DSMZ (Deutsche Sammlung von Mikroorganismen und Zellkulturen, www.dsmz.de/catalogues/catalogue-human-and-animal-cell-lines.html) (*62*). Tigecycline, doxorubicin, and venetoclax (all from Carbosynth) were dissolved in dimethyl sulfoxide and added directly to the culture medium. Staining for SA-βgal was performed

as described previously (*63*). Viable cell numbers were assessed by Trypan blue exclusion with an automated cell counter (TC20, Bio-Rad), following the manufacturer's instructions. Oxygen consumption of cultivated cells was determined by polarographic analysis using a Clark-type Hansatech Oxygraph in a 1-ml chamber. Drug synergies were evaluated using the ZIP model in SynergyFinder (*64*).

Immunoblot and immunohistological analysis

Immunoblot and immunohistological analysis were performed as described (*16*). The following primary antibodies were uses for immunoblotting: mouse monoclonal anti-vinculin (catalog #ab18058, Abcam), mouse monoclonal anti-COX1 (catalog # ab14705, Abcam), mouse monoclonal anti-COX2 (catalog #12C4F12, Invitrogen), mouse monoclonal anti-SDHA (catalog #459200, Invitrogen), rabbit monoclonal anti-MYC Y69 (catalog #GR144732-28, Abcam), rabbit monoclonal anti-BCL2 E17 (catalog #ab32124, Abcam), and mouse monoclonal anti-BCL2 [OP60] (Calbiochem). The failure of the OP60 antibody to recognize BCL2 in SU-DHL-6 cells (Fig. 2B) has been reported previously (*65*). For immunohistological detection of Ki-67 and cleaved caspase-3, we used antibodies #M7249 (Dako) and #9661 (Cell Signaling), respectively.

RNA extraction and analysis

Total RNA was purified and analyzed by RT-PCR (reverse transcription polymerase chain reaction), as described (*16*), with the following primers: human *MYC*, CTAGATGGCATCATTCTTCC and GAAACTGGGCAAACAACAC; human *BCL2*, CACGCTGGGAGAACAGGGTA and GGATGTACTTCATCACTATCTCCCG; mouse *Cdkn1a*, CTGGGAGGGGACAAGAG and GCTTGGAGTGATAGAAATCTG; human and mouse *RPLP0*, TTCATTGTGGGAGCAGAC and CAGCAGTTTCTCCAGAGC.

Flow cytometry

For DNA content analysis, cells were fixed with 70% EtOH, resuspended in phosphate-buffered saline with propidium iodide (50 μg/ml) and RNase A (40 μg/ml), and stained overnight at 4°C in the dark. Samples were acquired on a FACSCalibur flow cytometer (Becton Dickinson).

Peripheral blood profiles

For peripheral blood analysis, 50 μl of blood was collected by tail vein bleeding, and 10 μl of 0.5 M EDTA was immediately added to prevent coagulation. Whole blood was analyzed using a hematological analyzer (Beckman Dickinson). Alanine aminotransferase activity was assayed with a specific kit (MAK052, Sigma-Aldrich).

Xenograft models of human DLBCL

SU-DHL-6, DOHH-2, OCI-LY8, or OCI-LY7 cells (10^6) were transplanted subcutaneously in irradiated (3 gray) CD1-nude nu/nu female mice. Treatment started upon the appearance of measurable tumors. Tumor volumes were assessed from the start of the treatment every 2 days with a digital caliper and calculated as 1/2(length × width^2) (*66*). The following treatment schemes were used: twice a day intraperitoneal injection of tigecycline (spaced by ~8 hours) and/or daily oral gavage with venetoclax for 5 days, followed by 2 days off and a repeat of the same scheme, for a total of 12 days. A single intravenous injection of rituximab (10 mg/kg) was used for the experiment in fig. S9. For the experiment in fig. S5 (B and C), tigecycline was delivered with a single intravenous injection every 3 days, for a total of 12 days. Tigecycline was dissolved in saline solution (0.8% NaCl); venetoclax was dissolved in 60% Phosal 50 PG (Lipoid), 30% polyethylene glycol (Sigma-Aldrich), and 10% ethanol. Solutions were freshly prepared from dry powder just before each injection.

The PDX line DFBL-69487-V3-mCLP (*33*) was acquired from the Public Repository of Xenografts (www.proxe.org). Cells (10^6) were xenografted via tail vein injection into 6- to 8-week-old female NSG mice. The animals were monitored once a week by whole-body imaging on an IVIS Lumina III platform after intraperitoneal injection of XenoLight D-Luciferin (150 mg/kg) (#122799, PerkinElmer) and anesthesia with isoflurane. The data were analyzed with the Living Image software, version 4.2 (Caliper Life Sciences). Radiant efficiency was calculated on the basis of the epifluorescence signal, as indicated in the user manual. Experiments involving animals were carried out in accordance with the Italian Law D.lgs. 26/2014, which enforces Directive 2010/63/EU of the European Parliament and of the Council of 22 September 2010 on the protection of animals used for scientific purposes.

Statistics

All data are means ± SD. Statistical analyses were performed by unpaired two-tailed Student's *t* test. Differences were considered statistically significant at $P < 0.05$. Statistical evaluation of survival curves was performed using multiple *t* tests for each time point and the Holm-Sidak method.

SUPPLEMENTARY MATERIALS

www.sciencetranslationalmedicine.org/cgi/content/full/10/426/eaan8723/DC1
Fig. S1. Response of mouse Eμ-*myc*/*BCL2* lymphomas to tigecycline and venetoclax.
Fig. S2. Synergistic effects of tigecycline and venetoclax against human DHL cell lines.
Fig. S3. Similar effects of tigecycline, doxycycline, and tetracycline in DHL cells.
Fig. S4. Short-term effects of tigecycline and venetoclax in SU-DHL-6 tumors.
Fig. S5. Reactive liver lesions caused by intraperitoneal delivery of tigecycline.
Fig. S6. Toxicology of tigecycline and venetoclax drug combination studies in vivo.
Fig. S7. Whole-body imaging of PDX-derived tumors treated with tigecycline and/or venetoclax.
Fig. S8. Kaplan-Meier representation of disease-free survival in PDX-recipient mice.
Fig. S9. Effect of rituximab with tigecycline and/or venetoclax on DHL xenografts.
Fig. S10. Whole-body imaging of PDX-derived tumors treated with rituximab, tigecycline, and/or venetoclax.
Table S1. Primary data.

REFERENCES AND NOTES

1. S. H. Swerdlow, E. Campo, S. A. Pileri, N. Lee Harris, H. Stein, R. Siebert, R. Advani, M. Ghielmini, G. A. Salles, A. D. Zelenetz, E. S. Jaffe, The 2016 revision of the World Health Organization classification of lymphoid neoplasms. *Blood* **127**, 2375–2390 (2016).
2. P. Sesques, N. A. Johnson, Approach to the diagnosis and treatment of high-grade B-cell lymphomas with *MYC* and *BCL2* and/or *BCL6* rearrangements. *Blood* **129**, 280–288 (2017).
3. J. W. Friedberg, How I treat double-hit lymphoma. *Blood* **130**, 590–596 (2017).
4. Y. Khelfa, Y. Lebowicz, M. O. Jamil, Double-hit large B cell lymphoma. *Curr. Oncol. Rep.* **19**, 74 (2017).
5. C. Sarkozy, A. Traverse-Glehen, B. Coiffier, Double-hit and double-protein-expression lymphomas: Aggressive and refractory lymphomas. *Lancet Oncol.* **16**, e555–e567 (2015).
6. M. A. Anderson, A. Tsui, M. Wall, D. C. S. Huang, A. W. Roberts, Current challenges and novel treatment strategies in double hit lymphomas. *Ther. Adv. Hematol.* **7**, 52–64 (2016).
7. D. J. Landsburg, M. K. Falkiewicz, J. Maly, K. A. Blum, C. Howlett, T. Feldman, Outcomes of patients with double-hit lymphoma who achieve first complete remission. *J. Clin. Oncol.* **35**, 2260–2267 (2017).
8. A. J. Souers, J. D. Leverson, E. R. Boghaert, S. L. Ackler, N. D. Catron, J. Chen, B. D. Dayton, H. Ding, S. H. Enschede, W. J. Fairbrother, D. C. S. Huang, S. G. Hymowitz, S. Jin, S. Lin Khaw, P. J. Kovar, L. T. Lam, J. Lee, H. L. Maecker, K. C. Marsh, K. D. Mason, M. J. Mitten, P. M. Nimmer, A. Oleksijew, C. H. Park, C.-M. Park, D. C. Phillips, A. W. Roberts, D. Sampath, J. F. Seymour, M. L. Smith, G. M. Sullivan, S. K. Tahir, C. Tse, M. D. Wendt, Y. Xiao, J. C. Xue, H. Zhang, R. A. Humerickhouse, S. H. Rosenberg, S. W. Elmore, ABT-199,

a potent and selective BCL-2 inhibitor, achieves antitumor activity while sparing platelets. *Nat. Med.* **19**, 202–208 (2013).
9. J. D. Leverson, D. Sampath, A. J. Souers, S. H. Rosenberg, W. J. Fairbrother, M. Amiot, M. Konopleva, A. Letai, Found in translation: How preclinical research is guiding the clinical development of the BCL2-selective inhibitor venetoclax. *Cancer Discov.* **7**, 1376–1393 (2017).
10. A. Younes, S. Ansell, N. Fowler, W. Wilson, S. de Vos, J. Seymour, R. Advani, A. Forero, F. Morschhauser, M. Jose Kersten, K. Tobinai, P. Luigi Zinzani, E. Zucca, J. Abramson, J. Vose, The landscape of new drugs in lymphoma. *Nat. Rev. Clin. Oncol.* **14**, 335–346 (2017).
11. D. L. Vaux, S. Cory, J. M. Adams, *Bcl-2* gene promotes haemopoietic cell survival and cooperates with *c-myc* to immortalize pre-B cells. *Nature* **335**, 440–442 (1988).
12. A. Strasser, A. W. Harris, M. L. Bath, S. Cory, Novel primitive lymphoid tumours induced in transgenic mice by cooperation between *myc* and *bcl-2*. *Nature* **348**, 331–333 (1990).
13. A. Fanidi, E. A. Harrington, G. I. Evan, Cooperative interaction between *c-myc* and *bcl-2* proto-oncogenes. *Nature* **359**, 554–556 (1992).
14. R. P. Bissonnette, F. Echeverri, A. Mahboubi, D. R. Green, Apoptotic cell death induced by *c-myc* is inhibited by *bcl-2*. *Nature* **359**, 552–554 (1992).
15. A. R. D. Delbridge, S. Grabow, A. Strasser, D. L. Vaux, Thirty years of BCL-2: Translating cell death discoveries into novel cancer therapies. *Nat. Rev. Cancer* **16**, 99–109 (2016).
16. A. D'Andrea, I. Gritti, P. Nicoli, M. Giorgio, M. Doni, A. Conti, V. Bianchi, L. Casoli, A. Sabò, A. Mironov, G. V. Beznoussenko, B. Amati, The mitochondrial translation machinery as a therapeutic target in Myc-driven lymphomas. *Oncotarget* **7**, 72415–72430 (2016).
17. A. R. Oran, C. M. Adams, X.-Y. Zhang, V. J. Gennaro, H. K. Pfeiffer, H. S. Mellert, H. E. Seidel, K. Mascioli, J. Kaplan, M. R. Gaballa, C. Shen, I. Rigoutsos, M. P. King, J. L. Cotney, J. J. Arnold, S. D. Sharma, U. E. Martinez-Outschoorn, C. R. Vakoc, L. A. Chodosh, J. E. Thompson, J. E. Bradner, C. E. Cameron, G. S. Shadel, C. M. Eischen, S. B. McMahon, Multi-focal control of mitochondrial gene expression by oncogenic MYC provides potential therapeutic targets in cancer. *Oncotarget* **7**, 72395–72414 (2016).
18. Z. Xu, Y. Yan, Z. Li, L. Qian, Z. Gong, The antibiotic drug tigecycline: A focus on its promising anticancer properties. *Front. Pharmacol.* **7**, 473 (2016).
19. A. Sabò, T. R. Kress, M. Pelizzola, S. de Pretis, M. M. Gorski, A. Tesi, M. J. Morelli, P. Bora, M. Doni, A. Verrecchia, C. Tonelli, G. Fagà, V. Bianchi, A. Ronchi, D. Low, H. Müller, E. Guccione, S. Campaner, B. Amati, Selective transcriptional regulation by Myc in cellular growth control and lymphomagenesis. *Nature* **511**, 488–492 (2014).
20. J. R. Dörr, Y. Yu, M. Milanovic, G. Beuster, C. Zasada, J. H. M. Däbritz, J. Lisec, D. Lenze, A. Gerhardt, K. Schleicher, S. Kratzat, B. Purfürst, S. Walenta, W. Mueller-Klieser, M. Gräler, M. Hummel, U. Keller, A. K. Buck, B. Dörken, L. Willmitzer, M. Reimann, S. Kempa, S. Lee, C. A. Schmitt, Synthetic lethal metabolic targeting of cellular senescence in cancer therapy. *Nature* **501**, 421–425 (2013).
21. C. van den Bogert, B. H. J. Dontje, J. J. Wybenga, A. M. Kroon, Arrest of in vivo proliferation of Zajdela tumor cells by inhibition of mitochondrial protein synthesis. *Cancer Res.* **41**, 1943–1947 (1981).
22. A. M. Kroon, B. H. J. Dontje, M. Holtrop, C. Van Den Bogert, The mitochondrial genetic system as a target for chemotherapy: Tetracyclines as cytostatics. *Cancer Lett.* **25**, 33–40 (1984).
23. C. van den Bogert, B. H. Dontje, A. M. Kroon, The antitumour effect of doxycycline on a T-cell leukaemia in the rat. *Leuk. Res.* **9**, 617–623 (1985).
24. C. van den Bogert, B. H. J. Dontje, M. Holtrop, T. E. Melis, J. C. Romijn, J. W. van Dongen, A. M. Kroon, Arrest of the proliferation of renal and prostate carcinomas of human origin by inhibition of mitochondrial protein synthesis. *Cancer Res.* **46**, 3283–3289 (1986).
25. R. Lamb, B. Ozsvari, C. L. Lisanti, H. B. Tanowitz, A. Howell, U. E. Martinez-Outschoorn, F. Sotgia, M. P. Lisanti, Antibiotics that target mitochondria effectively eradicate cancer stem cells, across multiple tumor types: Treating cancer like an infectious disease. *Oncotarget* **6**, 4569–4584 (2015).
26. M. Škrtić, S. Sriskanthadevan, B. Jhas, M. Gebbia, X. Wang, Z. Wang, R. Hurren, Y. Jitkova, M. Gronda, N. Maclean, C. K. Lai, Y. Eberhard, J. Bartoszko, P. Spagnuolo, A. C. Rutledge, A. Datti, T. Ketela, J. Moffat, B. H. Robinson, J. H. Cameron, J. Wrana, C. J. Eaves, M. D. Minden, J. C. Y. Wang, J. E. Dick, K. Humphries, C. Nislow, G. Giaever, A. D. Schimmer, Inhibition of mitochondrial translation as a therapeutic strategy for human acute myeloid leukemia. *Cancer Cell* **20**, 674–688 (2011).
27. X. Jia, Z. Gu, W. Chen, J. Jiao, Tigecycline targets nonsmall cell lung cancer through inhibition of mitochondrial function. *Fundam. Clin. Pharmacol.* **30**, 297–306 (2016).
28. R. A. Jones, T. J. Robinson, J. C. Liu, M. Shrestha, V. Voisin, Y. Ju, P. E. D. Chung, G. Pellecchia, V. L. Fell, S. Bae, L. Muthuswamy, A. Datti, S. E. Egan, Z. Jiang, G. Leone, G. D. Bader, A. Schimmer, E. Zacksenhaus, RB1 deficiency in triple-negative breast cancer induces mitochondrial protein translation. *J. Clin. Invest.* **126**, 3739–3757 (2016).
29. J. Tan, M. Song, M. Zhou, Y. Hu, Antibiotic tigecycline enhances cisplatin activity against human hepatocellular carcinoma through inducing mitochondrial dysfunction and oxidative damage. *Biochem. Biophys. Res. Commun.* **483**, 17–23 (2017).
30. B. Wang, J. Ao, D. Yu, T. Rao, Y. Ruan, X. Yao, Inhibition of mitochondrial translation effectively sensitizes renal cell carcinoma to chemotherapy. *Biochem. Biophys. Res. Commun.* **490**, 767–773 (2017).
31. E. M. Kuntz, P. Baquero, A. M. Michie, K. Dunn, S. Tardito, T. L. Holyoake, G. V. Helgason, E. Gottlieb, Targeting mitochondrial oxidative phosphorylation eradicates therapy-resistant chronic myeloid leukemia stem cells. *Nat. Med.* **23**, 1234–1240 (2017).
32. G. A. Reed, G. J. Schiller, S. Kambhampati, M. S. Tallman, D. Douer, M. D. Minden, K. W. Yee, V. Gupta, J. Brandwein, Y. Jitkova, M. Gronda, R. Hurren, A. Shamas-Din, A. C. Schuh, A. D. Schimmer, A phase 1 study of intravenous infusions of tigecycline in patients with acute myeloid leukemia. *Cancer Med.* **5**, 3031–3040 (2016).
33. E. C. Townsend, M. A. Murakami, A. Christodoulou, A. L. Christie, J. Köster, T. A. DeSouza, E. A. Morgan, S. P. Kallgren, H. Liu, S.-C. Wu, O. Plana, J. Montero, K. E. Stevenson, P. Rao, R. Vadhi, M. Andreeff, P. Armand, K. K. Ballen, P. Barzaghi-Rinaudo, S. Cahill, R. A. Clark, V. G. Cooke, M. S. Davids, D. J. DeAngelo, D. M. Dorfman, H. Eaton, B. L. Ebert, J. Etchin, B. Firestone, D. C. Fisher, A. S. Freedman, I. A. Galinsky, H. Gao, J. S. Garcia, F. Garnache-Ottou, T. A. Graubert, A. Gutierrez, E. Halilovic, M. H. Harris, Z. T. Herbert, S. M. Horwitz, G. Inghirami, A. M. Intlekofer, M. Ito, S. Izraeli, E. D. Jacobsen, C. A. Jacobson, S. Jeay, I. Jeremias, M. A. Kelliher, R. Koch, M. Konopleva, N. Kopp, S. M. Kornblau, A. L. Kung, T. S. Kupper, N. R. LeBoeuf, A. S. LaCasce, E. Lees, L. S. Li, A. Thomas Look, M. Murakami, M. Muschen, D. Neuberg, S. Y. Ng, O. O. Odejide, S. H. Orkin, R. R. Paquette, A. E. Place, J. E. Roderick, J. A. Ryan, S. E. Sallan, B. Shoji, L. B. Silverman, R. J. Soiffer, D. P. Steensma, K. Stegmaier, R. M. Stone, J. Tamburini, A. R. Thorner, P. van Hummelen, M. Wadleigh, M. Wiesmann, A. P. Weng, J. U. Wuerthner, D. A. Williams, B. M. Wollison, A. A. Lane, A. Letai, M. M. Bertagnolli, J. Ritz, M. Brown, H. Long, J. C. Aster, M. A. Shipp, J. D. Griffin, D. M. Weinstock, The public repository of xenografts enables discovery and randomized phase II-like trials in mice. *Cancer Cell* **29**, 574–586 (2016).
34. H. Li, S. Jiao, X. Li, H. Banu, S. Hamal, X. Wang, Therapeutic effects of antibiotic drug tigecycline against cervical squamous cell carcinoma by inhibiting Wnt/β-catenin signaling. *Biochem. Biophys. Res. Commun.* **467**, 14–20 (2015).
35. X. Zhong, E. Zhao, C. Tang, W. Zhang, J. Tan, Z. Dong, H.-F. Ding, H. Cui, Antibiotic drug tigecycline reduces neuroblastoma cells proliferation by inhibiting Akt activation in vitro and in vivo. *Tumour Biol.* **37**, 7615–7623 (2016).
36. Z. Lu, N. Xu, B. He, C. Pan, Y. Lan, H. Zhou, X. Liu, Inhibition of autophagy enhances the selective anti-cancer activity of tigecycline to overcome drug resistance in the treatment of chronic myeloid leukemia. *J. Exp. Clin. Cancer Res.* **36**, 43 (2017).
37. C. Tang, L. Yang, X. Jiang, C. Xu, M. Wang, Q. Wang, Z. Zhou, Z. Xiang, H. Cui, Antibiotic drug tigecycline inhibited cell proliferation and induced autophagy in gastric cancer cells. *Biochem. Biophys. Res. Commun.* **446**, 105–112 (2014).
38. B. Ozsvari, M. Fiorillo, G. Bonuccelli, A. R. Cappello, L. Frattaruolo, F. Sotgia, R. Trowbridge, R. Foster, M. P. Lisanti, Mitoriboscins: Mitochondrial-based therapeutics targeting cancer stem cells (CSCs), bacteria and pathogenic yeast. *Oncotarget* **8**, 67457–67472 (2017).
39. E. Norberg, A. Lako, P.-H. Chen, I. A. Stanley, F. Zhou, S. B. Ficarro, B. Chapuy, L. Chen, S. Rodig, D. Shin, D. Wook Choi, S. Lee, M. A. Shipp, J. A. Marto, N. N. Danial, Differential contribution of the mitochondrial translation pathway to the survival of diffuse large B-cell lymphoma subsets. *Cell Death Differ.* **24**, 251–262 (2017).
40. S. Monti, K. J. Savage, J. L. Kutok, F. Feuerhake, P. Kurtin, M. Mihm, B. Wu, L. Pasqualucci, D. Neuberg, R. C. T. Aguiar, P. Dal Cin, C. Ladd, G. S. Pinkus, G. Salles, N. L. Harris, R. Dalla-Favera, T. M. Habermann, J. C. Aster, T. R. Golub, M. A. Shipp, Molecular profiling of diffuse large B-cell lymphoma identifies robust subtypes including one characterized by host inflammatory response. *Blood* **105**, 1851–1861 (2005).
41. G. Wright, B. Tan, A. Rosenwald, E. H. Hurt, A. Wiestner, L. M. Staudt, A gene expression-based method to diagnose clinically distinct subgroups of diffuse large B cell lymphoma. *Proc. Natl. Acad. Sci. U.S.A.* **100**, 9991–9996 (2003).
42. A. Reddy, J. Zhang, N. S. Davis, A. B. Moffitt, C. L. Love, A. Waldrop, S. Leppa, A. Pasanen, L. Meriranta, M.-L. Karjalainen-Lindsberg, P. Nørgaard, M. Pedersen, A. O. Gang, E. Høgdall, T. B. Heavican, W. Lone, J. Iqbal, Q. Qin, G. Li, S. Young Kim, J. Healy, K. L. Richards, Y. Fedoriw, L. Bernal-Mizrachi, J. L. Koff, A. D. Staton, C. R. Flowers, O. Paltiel, N. Goldschmidt, M. Calaminici, A. Clear, J. Gribben, E. Nguyen, M. B. Czader, S. L. Ondrejka, A. Collie, E. D. Hsi, E. Tse, R. K. H. Au-Yeung, Y.-L. Kwong, G. Srivastava, W. W. L. Choi, A. M. Evens, M. Pilichowska, M. Sengar, N. Reddy, S. Li, A. Chadburn, L. I. Gordon, E. S. Jaffe, S. Levy, R. Rempel, T. Tzeng, L. E. Happ, T. Dave, D. Rajagopalan, J. Datta, D. B. Dunson, S. S. Dave, Genetic and functional drivers of diffuse large B cell lymphoma. *Cell* **171**, 481–494 (2017).
43. R. F. Chemaly, S. S. Hanmod, Y. Jiang, D. B. Rathod, V. Mulanovich, J. A. Adachi, K. V. Rolston, I. I. Raad, R. Y. Hachem, Tigecycline use in cancer patients with serious infections: A report on 110 cases from a single institution. *Medicine* **88**, 211–220 (2009).
44. C. I. Kosmidis, P. H. Chandrasekar, Management of gram-positive bacterial infections in patients with cancer. *Leuk. Lymphoma* **53**, 8–18 (2012).
45. K. S. Schwab, C. Hahn-Ast, W. J. Heinz, U. Germing, G. Egerer, A. Glasmacher, C. Leyendecker, G. Marklein, C. M. Nellessen, P. Brossart, M. von Lilienfeld-Toal, Tigecycline in febrile neutropenic patients with haematological malignancies: A retrospective case documentation in four university hospitals. *Infection* **42**, 97–104 (2014).

46. G. Bucaneve, A. Micozzi, M. Picardi, S. Ballanti, N. Cascavilla, P. Salutari, G. Specchia, R. Fanci, M. Luppi, L. Cudillo, R. Cantaffa, G. Milone, M. Bocchia, G. Martinelli, M. Offidani, A. Chierichini, F. Fabbiano, G. Quarta, V. Primon, B. Martino, A. Manna, E. Zuffa, A. Ferrari, G. Gentile, R. Foà, A. Del Favero, Results of a multicenter, controlled, randomized clinical trial evaluating the combination of piperacillin/tazobactam and tigecycline in high-risk hematologic patients with cancer with febrile neutropenia. *J. Clin. Oncol.* **32**, 1463–1471 (2014).
47. K. V. I. Rolston, M. A. Jamal, L. Nesher, S. A. Shelburne, I. Raad, R. A. Prince, In vitro activity of ceftaroline and comparator agents against Gram-positive and Gram-negative clinical isolates from cancer patients. *Int. J. Antimicrob. Agents* **49**, 416–421 (2017).
48. A. D. Schimmer, M. Škrtić, Therapeutic potential of mitochondrial translation inhibition for treatment of acute myeloid leukemia. *Expert Rev. Hematol.* **5**, 117–119 (2012).
49. Y. Jitkova, M. Gronda, R. Hurren, X. Wang, C. A. Goard, B. Jhas, A. D. Schimmer, A novel formulation of tigecycline has enhanced stability and sustained antibacterial and antileukemic activity. *PLOS ONE* **9**, e95281 (2014).
50. B. Z. Carter, P. Y. Mak, H. Mu, H. Zhou, D. H. Mak, W. Schober, J. D. Leverson, B. Zhang, R. Bhatia, X. Huang, J. Cortes, H. Kantarjian, M. Konopleva, M. Andreeff, Combined targeting of BCL-2 and BCR-ABL tyrosine kinase eradicates chronic myeloid leukemia stem cells. *Sci. Transl. Med.* **8**, 355ra117 (2016).
51. T. K. Ko, C. T. H. Chuah, J. W. J. Huang, K.-P. Ng, S. T. Ong, The BCL2 inhibitor ABT-199 significantly enhances imatinib-induced cell death in chronic myeloid leukemia progenitors. *Oncotarget* **5**, 9033–9038 (2014).
52. A. Viale, P. Pettazzoni, C. A. Lyssiotis, H. Ying, N. Sánchez, M. Marchesini, A. Carugo, T. Green, S. Seth, V. Giuliani, M. Kost-Alimova, F. Muller, S. Colla, L. Nezi, G. Genovese, A. K. Deem, A. Kapoor, W. Yao, E. Brunetto, Y. Kang, M. Yuan, J. M. Asara, Y. A. Wang, T. P. Heffernan, A. C. Kimmelman, H. Wang, J. B. Fleming, L. C. Cantley, R. A. DePinho, G. F. Draetta, Oncogene ablation-resistant pancreatic cancer cells depend on mitochondrial function. *Nature* **514**, 628–632 (2014).
53. E. D. Lagadinou, A. Sach, K. Callahan, R. M. Rossi, S. J. Neering, M. Minhajuddin, J. M. Ashton, S. Pei, V. Grose, K. M. O'Dwyer, J. L. Liesveld, P. S. Brookes, M. W. Becker, C. T. Jordan, BCL-2 inhibition targets oxidative phosphorylation and selectively eradicates quiescent human leukemia stem cells. *Cell Stem Cell* **12**, 329–341 (2013).
54. J. Velez, R. Pan, J. T. C. Lee, L. Enciso, M. Suarez, J. E. Duque, D. Jaramillo, C. Lopez, L. Morales, W. Bornmann, M. Konopleva, G. Krystal, M. Andreeff, I. Samudio, Biguanides sensitize leukemia cells to ABT-737-induced apoptosis by inhibiting mitochondrial electron transport. *Oncotarget* **7**, 51435–51449 (2016).
55. K.-m. Lee, J. M. Giltnane, J. M. Balko, L. J. Schwarz, A. L. Guerrero-Zotano, K. E. Hutchinson, M. J. Nixon, M. V. Estrada, V. Sánchez, M. E. Sanders, T. Lee, H. Gómez, A. Lluch, J. A. Pérez-Fidalgo, M. M. Wolf, G. Andrejeva, J. C. Rathmell, S. W. Fesik, C. L. Arteaga, MYC and MCL1 cooperatively promote chemotherapy-resistant breast cancer stem cells via regulation of mitochondrial oxidative phosphorylation. *Cell Metab.* **26**, 633–647.e7 (2017).
56. S. Stilgenbauer, B. Eichhorst, J. Schetelig, S. Coutre, J. F. Seymour, T. Munir, S. D. Puvvada, C.-M. Wendtner, A. W. Roberts, W. Jurczak, S. P. Mulligan, S. Böttcher, M. Mobasher, M. Zhu, M. Desai, B. Chyla, M. Verdugo, S. H. Enschede, E. Cerri, R. Humerickhouse, G. Gordon, M. Hallek, W. G. Wierda, Venetoclax in relapsed or refractory chronic lymphocytic leukaemia with 17p deletion: A multicentre, open-label, phase 2 study. *Lancet Oncol.* **17**, 768–778 (2016).
57. M. S. Davids, A. W. Roberts, J. F. Seymour, J. M. Pagel, B. S. Kahl, W. G. Wierda, S. Puvvada, T. J. Kipps, M. A. Anderson, A. H. Salem, M. Dunbar, M. Zhu, F. Peale, J. A. Ross, L. Gressick, M. Desai, S. Y. Kim, M. Verdugo, R. A. Humerickhouse, G. B. Gordon, J. F. Gerecitano, Phase I first-in-human study of venetoclax in patients with relapsed or refractory non-Hodgkin lymphoma. *J. Clin. Oncol.* **35**, 826–833 (2017).
58. J. F. Seymour, S. Ma, D. M. Brander, M. Y. Choi, J. Barrientos, M. S. Davids, M. A. Anderson, A. W. Beaven, S. T. Rosen, C. S. Tam, B. Prine, S. K. Agarwal, W. Munasinghe, M. Zhu, L. L. Lash, M. Desai, E. Cerri, M. Verdugo, S. Y. Kim, R. A. Humerickhouse, G. B. Gordon, T. J. Kipps, A. W. Roberts, Venetoclax plus rituximab in relapsed or refractory chronic lymphocytic leukaemia: A phase 1b study. *Lancet Oncol.* **18**, 230–240 (2017).
59. A. W. Roberts, Targeting apoptotic pathways to treat lymphoid malignancies. *Rinsho Ketsueki* **57**, 2054–2058 (2016).
60. S. Cang, C. Iragavarapu, J. Savooji, Y. Song, D. Liu, ABT-199 (venetoclax) and BCL-2 inhibitors in clinical development. *J. Hematol. Oncol.* **8**, 129 (2015).
61. K. J. Freise, A. K. Jones, R. M. Menon, M. E. Verdugo, R. A. Humerickhouse, W. M. Awni, A. H. Salem, Relationship between venetoclax exposure, rituximab coadministration, and progression-free survival in patients with relapsed or refractory chronic lymphocytic leukemia: Demonstration of synergy. *Hematol. Oncol.* **35**, 679–684 (2017).
62. H. G. Drexler, S. Eberth, S. Nagel, R. A. F. MacLeod, Malignant hematopoietic cell lines: In vitro models for double-hit B-cell lymphomas. *Leuk. Lymphoma* **57**, 1015–1020 (2016).
63. G. P. Dimri, X. Lee, G. Basile, M. Acosta, G. Scott, C. Roskelley, E. E. Medrano, M. Linskens, I. Rubelj, O. Pereira-Smith, M. Peacocke, J. Campisi, A biomarker that identifies senescent human cells in culture and in aging skin in vivo. *Proc. Natl. Acad. Sci. U.S.A.* **92**, 9363–9367 (1995).
64. A. Ianevski, L. He, T. Aittokallio, J. Tang, SynergyFinder: A web application for analyzing drug combination dose-response matrix data. *Bioinformatics* **33**, 2413–2415 (2017).
65. N. Masir, L. J. Campbell, M. Jones, D. Y. Mason, Pseudonegative BCL2 protein expression in a t(14;18) translocation positive lymphoma cell line: A need for an alternative BCL2 antibody. *Pathology* **42**, 212–216 (2010).
66. M. M. Jensen, J. T. Jørgensen, T. Binderup, A. Kjær, Tumor volume in subcutaneous mouse xenografts measured by microCT is more accurate and reproducible than determined by ^{18}F-FDG-microPET or external caliper. *BMC Med. Imaging* **8**, 16 (2008).

Acknowledgments: We thank A. Gobbi and M. Capillo for the help with the management of mouse colonies; F. Pisati for the preparation of histological samples; A. Christie, E. Battistello, and E. Oricchio for the biological samples; and D. Bellomo, A. Bisso, S. Campaner, L. Chierico, E. Derenzini, J. Franchini, M. Fumagalli, S. Minucci, G. Natoli, P.-G. Pelicci, A. Sabò, S. Pileri, and C. Tarella for the advice, comments, and discussions. **Funding:** This work was supported by grants from the European Research Council (grant agreement no. 268671-MYCNEXT), the Italian Health Ministry (RF-2011-02346976), and the Italian Association for Cancer Research (2012-13182 and 2015-16768) to B.A. A.D. was supported by a postdoctoral fellowship from the Fondazione Umberto Veronesi. **Author contributions:** M.R. and A.D. performed most of the experiments shown in this work, with the help of P.N., I.G., G.D., M.D., and M.G. D.O. provided the histopathological analysis. B.A. supervised the project and wrote the manuscript. **Competing interests:** This work has been the basis of patent application N. EP17169829.3 with the title "Combination of Tigecycline and a BCL-2 inhibitor and uses thereof" to the European Patent Office, filed on 5 May 2017 (inventors: B.A., M.R., and A.D.). **Data and materials availability:** The PDX line used in this work is covered by a material transfer agreement from the Dana Farber Cancer Institute to the Istituto Europeo di Oncologia (DFCI agreement no. A09770).

Submitted 31 May 2017
Resubmitted 8 November 2017
Accepted 28 December 2017
Published 31 January 2018
10.1126/scitranslmed.aan8723

Citation: M. Ravà, A. D'Andrea, P. Nicoli, I. Gritti, G. Donati, M. Doni, M. Giorgio, D. Olivero, B. Amati, Therapeutic synergy between tigecycline and venetoclax in a preclinical model of *MYC*/*BCL2* double-hit B cell lymphoma. *Sci. Transl. Med.* **10**, eaan8723 (2018).

Science Translational Medicine

Therapeutic synergy between tigecycline and venetoclax in a preclinical model of *MYCl BCL2* double-hit B cell lymphoma

Micol Ravà, Aleco D'Andrea, Paola Nicoli, Ilaria Gritti, Giulio Donati, Mirko Doni, Marco Giorgio, Daniela Olivero and Bruno Amati

Sci Transl Med **10**, eaan8723.
DOI: 10.1126/scitranslmed.aan8723

Doubling up against double-hit lymphoma

Double-hit lymphomas, a type of B cell lymphomas with concurrent activation of the *MYC* and *BCL2* oncogenes, are aggressive and difficult-to-treat tumors. In light of evidence showing that tigecycline, an antibiotic, may be effective against MYC-driven lymphomas, Ravà *et al*. combined it with venetoclax, a BCL2 inhibitor, to target the double-hit tumors. The authors found that the pair of clinically approved drugs showed synergy against the cancer and was also effective in combination with rituximab, a mainstay of current treatment for lymphoma.